Phase Interactions and Structure Evolution of Heterophasic Ethylene–Propylene Copolymers as a Function of System Composition

P. Doshev,[1] G. Lohse,[2] S. Henning,[1] M. Krumova,[1] A. Heuvelsland,[2] G. Michler,[1] H.-J. Radusch[1]

[1]*Institute of Materials Science, Martin Luther University Halle-Wittenberg, D-06099 Halle (Saale), Germany*
[2]*Dow Olefinverbund GmbH, D-06258 Schkopau, Germany*

Received 1 June 2005; accepted 11 August 2005
DOI 10.1002/app.22921
Published online in Wiley InterScience (www.interscience.wiley.com).

ABSTRACT: Heterophasic copolymers comprised of polypropylene (PP) matrix and ethylene–propylene copolymer (EPC) dispersed phase were investigated with respect to the dispersed phase composition, i.e., ethylene/propylene ratio. The rheological properties, morphology, as well as thermal and mechanical relaxation behavior were studied to describe the structure evolution and phase interactions between the components of the PP copolymers. Decrease of the ethylene content of the EPC leads to a higher matrix-dispersed phase compatibility, as evaluated by the shift of the glass transition temperatures of EPC and PP towards each other. At ethylene content of EPC of 17 wt %, the glass transition temperatures of the both phases merged into a joint relaxation. The effect of the EPC composition on the internal structure of the dispersed domains and on the morphology development of the heterophasic copolymers was demonstrated. Decreasing ethylene content was found to induce a refinement of the dispersed phase with several orders of magnitude down to 0.18 μm for propylene-rich EPC. Optical microscopy observations showed that the dispersed propylene-rich phase is preferably rejected at the interlamellar regions of the spherulites and/or at the interspherulitic regions, while the ethylene-rich domains are engulfed within the PP spherulites. Both of these processes impose an additional energetic barrier and influence the spherulite growth rate of the heterophasic materials. © 2006 Wiley Periodicals, Inc. J Appl Polym Sci 101: 2825–2837, 2006

Key words: polypropylene reactor blends; ethylene–propylene copolymer; compatibility; glass transition; morphology

INTRODUCTION

Polypropylene (PP) exhibits (along with a variety of useful properties) intrinsically brittle behavior under mechanical loading even above its glass transition temperature (T_g) and especially at low temperatures and high loading rates. Impact modification via downstream copolymerization of ethylene and propylene at a certain ratio of the components directly in a reactor cascade is a commercially effective practice to improve the toughness of PP.[1–2] So-produced heterophasic copolymers are also designated as reactor blends or impact modified PP. In comparison to the mechanical blends, the structure of the reactor blends was shown to be rather complex and its quantification involves an utilization of fractionation techniques such as temperature rising elution fractionation[3–6] or appropriate solvent fractionation[7] and a subsequent characterization of the fractions. It has been demonstrated that besides the PP matrix and the amorphous ethylene–propylene copolymer (aEPC), the reactor blends could comprise also an apparent spectrum of crystallizable copolymers of ethylene and propylene (cEPC). The presence of a cEPC fraction is favored both at high ethylene and high propylene containing EPC exhibiting a PE-like and PP-like crystallinity, respectively. The composition heterogeneity of the EPC phase in the reactor blends is assumed to be caused by the different reactivity of the monomers towards the diverse types of active sites existing in the Ziegler–Natta catalysts.[8] In fact, this heterogeneous structure can be considered advantageous for the interfacial adhesion and phase interactions between the components of the reactor blend, because of the compatibilization effect that some propylene-rich fractions may perform.[9–11]

The dispersed phase composition is recognized as a main parameter governing the matrix-dispersed phase interaction and the interfacial adhesion of blends of PP and ethylene-α-olefin copolymers. Yamaguchi et al.[12,13] reported that an increase of the comonomer content from ~30 to ~60 mol % leads to a significant enhancement of the matrix-dispersed phase compatibility in PP/ethylene-1-hexene and PP/ethylene-1-

Correspondence to: H.-J. Radusch (hans-joachim.radusch@iw.uni-halle.de).

Contract grant sponsors: State Government of Saxony-Anhalt; Dow Olefinverbund GmbH (Schkopau, Germany).

TABLE I
Material Characteristics

Materials	MFR^{PP} (g/10 min)	MFR^{Blend} (g/10 min)	XS (wt %)	$[\eta]^{EPC}$ (dL/g)	E_C^{EPC} (wt %)
PP	~20	20.0	—	1.5	—
PP/EP82	~20	4.7	20.4	3.4	82
PP/EP70	~20	8.1	20.5	2.4	70
PP/EP50	~20	9.4	20.3	2.5	50
PP/EP30	~20	11.1	19.2	2.4	30
PP/EP17	~20	9.7	25.2	1.6	17

butene blends. It was suggested that the comonomer-rich copolymers are miscible with iPP in the melt as well as with the amorphous region between the PP lamellae in the solid state. This suggestion was supported by rheological investigations, the raise of the long period as well as by the merging of the glass transition temperatures of the components.

The thermodynamic miscibility of blends of PP with propylene-rich EPC was investigated[14,15] by means of small angle neutron scattering. Lohse[14] reported that these blends are immiscible also in the melt (200°C), even when the ethylene content of the copolymer is as low as 8 wt %. On the other hand, Seki et al.[15] quoted that blends of PP and metallocene-catalyzed EPC containing 19 mol % as well as 47 mol % of deuterated ethylene units form a homogeneous mixture in the melt. However, phase separation was commonly observed by moderate cooling of the blend below the crystallization temperature of PP.[14,15] The effect of copolymer composition on the phase structure and mechanical property profile of PP/EPC has been the subject of several studies.[16–21] However, a systematic variation of the EPC ethylene content in mechanical PP/EPC blends over a wide concentration range was performed only by Greco et al.[16,17] and most recently by Nitta et al.[21] The disadvantageous form of the high comonomer containing ethylene-α-olefin copolymers (sticky or even resinous mass) permits only a discontinuous blending process performed in internal mixer[16,17] or by solution blending.[21] On the other hand, the *in reactor* blending technique offers a very effective and commercially relevant alternative. Proper control of the polymerization process enables the production of PP/EPC materials over a wide range of EPC composition directly in the reactor cascade. Some of the properties of PP/EPC *in situ* blends as influenced by the EPC composition are revealed by Van der Ven.[20] However, there is a lack of systematic investigation in this area.

The present work encompasses the effect of EPC composition on the phase behavior and morphology development of in reactor-produced PP/EPC blends. The results were discussed from the aspect of matrix-dispersed phase interactions and EPC microstructure evolution. The effect of the EPC composition on the rheological and thermal behavior of the PP-based reactor blends was demonstrated.

EXPERIMENTAL

Materials

The heterophasic copolymers used in this study were research materials provided by Dow Chemical (Schkopau, Germany). They were produced via sequential polymerization process in a batch reactor. In the first step, a PP homopolymer was produced in a liquid propylene reaction medium, followed by a gas phase copolymerization of propylene and ethylene at a certain ratio to form the dispersed EPC phase. The polymerization was carried out in the presence of a commercial fourth generation Ziegler–Natta catalyst system. The catalyst system consists of a titanium compound supported on a spherical $MgCl_2$ in combination with aluminum triethyl as a cocatalyst. Additionally, an external donor was used for isotacticity control. After the synthesis step, the materials were compounded with antioxidants and stabilizers in a single screw extruder PlastiCorder PL 2000 (Brabender) at 100 rpm and barrel zone temperatures from 210 to 230°C. The test specimens were produced using an injection molding machine BA 100 (Battenfeld) at a barrel temperature of 200°C and a mold temperature of 40°C. The main characteristics of the materials are summarized in Table I.

The PP homopolymer sample included in Table I is obtained by running only the homopolymer stage in the batch reactor at the same homopolymerization conditions as by the heterophasic copolymers and represents the PP matrix. The molecular parameters of the PP matrix as reflected by the MFR^{PP} were kept constant within the series. For the utilized catalyst system and polymerization procedure, a calibration curve exists between the PP melt flow rate and the weight average molecular weight (M_w^{PP}), as revealed in Figure 1. The calibration curve was derived by measuring a statistically secured number of PP homopolymers with known MFRs in gel permeation chromatography (GPC).

The EPC composition was characterized by the ethylene content of EPC (E_c^{EPC}). The E_c^{EPC} represents the

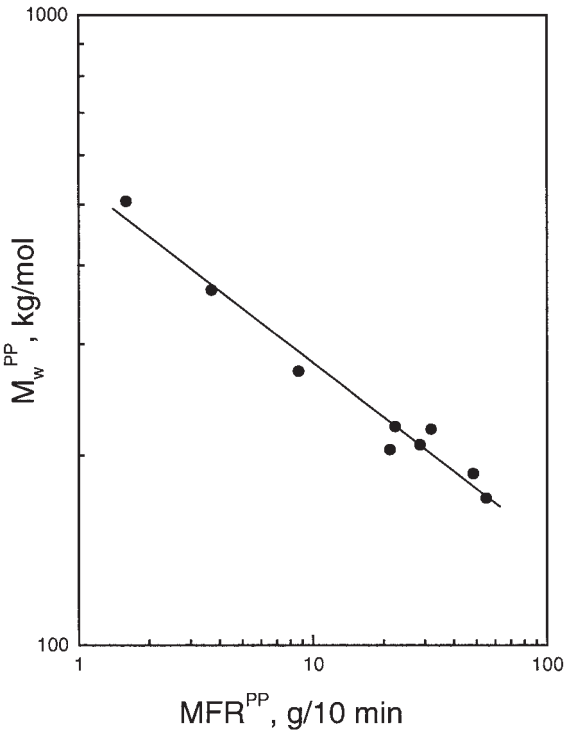

Figure 1 Correlation between the melt flow rate of the PP matrix (MFR^{PP}) and the weight average molecular weight (M_w^{PP}).

weight percent of ethylene in the gas phase reactor as determined by gas chromatography.

A known constraint of the *in reactor* blending process is that the amount of the elastomer phase incorporated cannot be controlled directly. In the present work, the amount of xylene soluble fraction (XS) was used as a qualitative measure of the elastomer loading. For the determination of the XS value, the sample was first dissolved in boiling xylene, and after cooling, precipitated with acetone to exclude the low isotacticity matrix fraction. The measurements were performed according to ASTM D 5492. The so-conducted fractionation gives rise to two main fractions: a xylene soluble and a xylene insoluble (XI) one. The XS fraction was taken as an illustration of the amount of EPC. However, it should be mentioned that XS does not register the amount of cEPC fragments, which are present at very low and very high ethylene contents. These fractions reside together with the PP matrix in the XI fraction. This fact would lead to a certain underestimation of the elastomer loading as revealed by XS in the materials of very low and very high ethylene contents.

The molecular parameters of the EPC are represented by the intrinsic viscosity ($[\eta]^{EPC}$). It was measured on the XS fraction in decaline at 135°C. Similar to the PP homopolymer, a calibration curve exists for the utilized catalyst system and polymerization procedure between $[\eta]^{EPC}$ values and M_w^{EPC} as determined by GPC (Fig. 2).

Characterization methods

Rheological investigation

The rheological properties of the materials were investigated via a rotational rheometer, type ARES (Rheometric Scientific) with plate–plate geometry. The measurements were performed at 190°C under nitrogen atmosphere in a frequency range from 0.1 to 250 rad/s and deformation amplitude of 10%. Assuming the validity of Cox-Merz relation ($\eta(\dot{\gamma}) = \eta^*(\omega)$ for $\dot{\gamma} = \omega$), the zero shear viscosities of the reactor blends were calculated using the Carreau-Yasuda model,[22] according to eq. (1)

$$\eta = \eta_0[1 + (\lambda\dot{\gamma})^a]^{\frac{(n-1)}{a}} \quad (1)$$

where η_0 is the zero shear viscosity, λ the characteristic relaxation time, and n the power-law index in the high frequency range. The parameter a describes the transition zone between the viscosity plateau and the power-law region.

Thermal properties

The thermal behavior of the reactor blends was examined by means of a differential scanning calorimeter

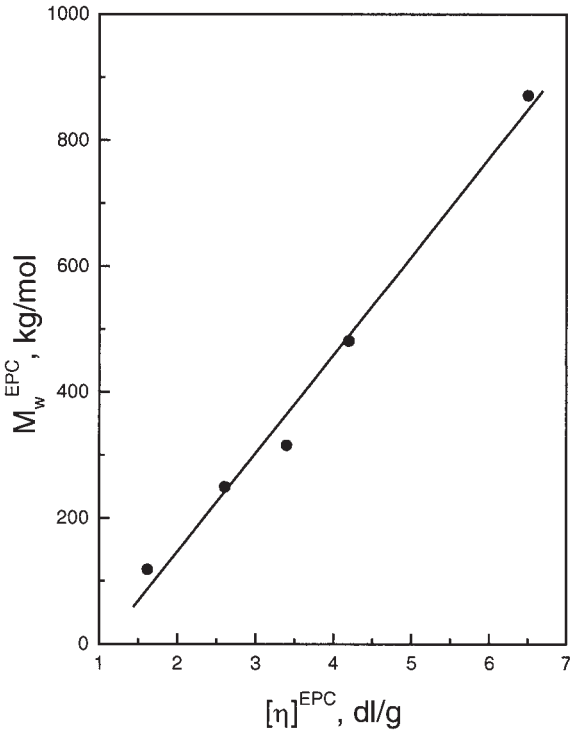

Figure 2 Correlation between the intrinsic viscosity of the EPC ($[\eta]^{EPC}$) and the weight average molecular weight (M_w^{EPC}).

DSC 820 (Mettler-Toledo). The samples were first heated to 230°C, kept at that temperature for 5 min to erase any thermal history, then cooled to −80°C at a cooling rate of 5 K/min, and reheated to 230°C at a rate of 10 K/min. The melting temperature (T_m) and the enthalpy of fusion (ΔH_f) of the materials were determined from the second heating and the crystallization temperatures (T_c) from the first cooling. The crystallinity of the PP matrix (X_c^{PP}) was calculated according to eq. (2)

$$X_c^{PP} = (\Delta H_f^{PP} / \Delta H_f^{0\,PP})\ 100\% \quad (2)$$

where $\Delta H^{PP}{}_f$ is the enthalpy of fusion of the PP phase of heterophasic copolymers and $\Delta H^{0\,PP}_f$ is the enthalpy of fusion of 100% crystalline iPP (209 J/g).[23]

The spherulite development under isothermal conditions was investigated by means of a polarized optical microscope DM-RX (Leica) equipped with a hotstage 1350 (Leitz). Sections of 10 μm thickness, obtained via a rotational microtome, were heated to 210°C, kept at that temperature for 5 min, and then cooled to a predetermined crystallization temperature T_c. The spherulite growth rate (G^{PP}) was calculated from the spherulite radius versus time curve. From three to six spherulites were considered for a given T_c and the average value of G^{PP} was derived.

Dynamic mechanical analysis

The mechanical relaxation behavior of the reactor blends as well as the glass transition temperatures of the components was characterized by means of a dynamic mechanical analyzer Mark III (Rheometric Scientific). Rectangular bars with geometry 40 × 10 × 4 mm were tested using a torsion pendulum at a frequency of 1 Hz and a heating rate of 1 K/min. The storage (G') and loss modulus (G'') as well as the loss factor (tan δ) were determined in the temperature range of −100 to 150°C. The tan δ curve was used for defining the glass transition temperatures of the components.

Morphology characterization

Morphology observations were accomplished by means of a scanning electron microscope (SEM) JSM 6300 (Jeol). Sections were cut from the core region of the injection molded dumbbell specimens via rotational microtome. Subsequently, the sections were subjected to a permanganic etching procedure according to Ref. 24 and gold-coated. The number (D_n) and weight (D_w) average particle diameters as well as the maximum particle diameter (D_{max}) were evaluated from the micrographs by means of image analyzing software QWin (Leica). A statistically secured number of particles have been considered at different magnifications. The calculations of D_n and D_w were accomplished according to eq. (3)

$$D_n = \frac{\sum_{i=1}^{N} n_i D_i}{\sum_{i=1}^{N} n_i} \qquad D_w = \frac{\sum_{i=1}^{N} n_i D_i^2}{\sum_{i=1}^{N} n_i D_i} \quad (3)$$

Transmission electron micrographs were obtained by means of a JEM 2010 device (JEOL), operated at 200 kV acceleration voltage. First, samples were exposed to RuO_4 vapor for contrast enhancement. The morphology investigation was performed on ultra-thin sections of 70 nm cut from the stained blocks at −100°C using a diamond knife equipped ultramicrotome MT-7 (RMC).

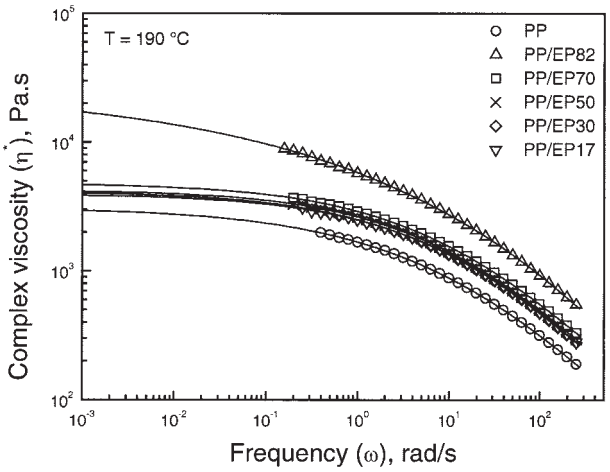

Figure 3 Complex viscosity (η^*) of neat PP and PP/EPC reactor blends as a function of frequency and EPC composition. Solid lines represent the Carreau-Yasuda model fits.

RESULTS AND DISCUSSION

Rheological properties

Figure 3 reveals the complex viscosity and the correspondent Carreau-Yasuda fits of the heterophasic copolymers as a function of frequency and ethylene content of EPC.

The utilized parameters for the Carreau-Yasuda model are reported in Table II.

Generally, the viscosity of the EPCs is much higher than that of the neat PP, leading to a higher viscosity of the reactor blends with respect to the matrix. Further on, an increase of the complex and the zero shear viscosity of the heterophasic copolymers was observed with increasing ethylene content of the EPC. The effect is combined with a shifting of the Newto-

TABLE II
Carreau-Yasuda Model Parameters

Materials	η_0 (Pa.s)	λ	a	n
PP	3095	0.0678	0.3878	0.219
PP/EP82	26090	2.99×10^{-5}	0.191	−1.236
PP/EP70	4788	0.1041	0.447	0.285
PP/EP50	4257	0.1037	0.457	0.280
PP/EP30	4136	0.083	0.440	0.246
PP/EPI7	3952	0.0753	0.451	0.238

nian plateau to lower frequencies.[25,26] Indeed, the Newtonian plateau of the ethylene-rich materials, namely the PP/EP82, cannot be measured directly at the applied deformation rate range. This leads to an underestimation of the characteristic relaxation time as well as to a much higher value of the extrapolated zero shear viscosity as indicated in Table II.

Taking into account that for the materials studied both the matrix viscosity and the XS amount were not considerably varied, the demonstrated raise of the complex and zero shear viscosity was attributed to the increased viscosity of the EPC dispersed phase with increasing ethylene content. This is in accordance with the study of Mighri et al.[26] where a strong increase of the complex and zero shear viscosity of neat EPCs were shown with increasing ethylene content. The effect was reasonably well described by means of the Tsenglou model.[27] The dynamic storage modulus of the heterophasic copolymers was also found to increase as a function of the ethylene content of the EPC as demonstrated in Figure 4.

However, while the rheological parameters of majority of the studied reactor blends lay within the same range, the material PP/EP82 exhibits a significantly higher viscosity as well as storage and loss modulus values. This behavior is assumed to be a complex

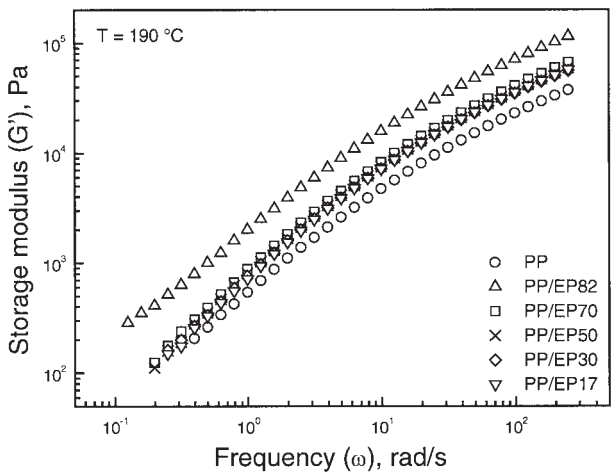

Figure 4 Storage modulus (G') of neat PP and PP/EPC as a function of frequency and EPC composition.

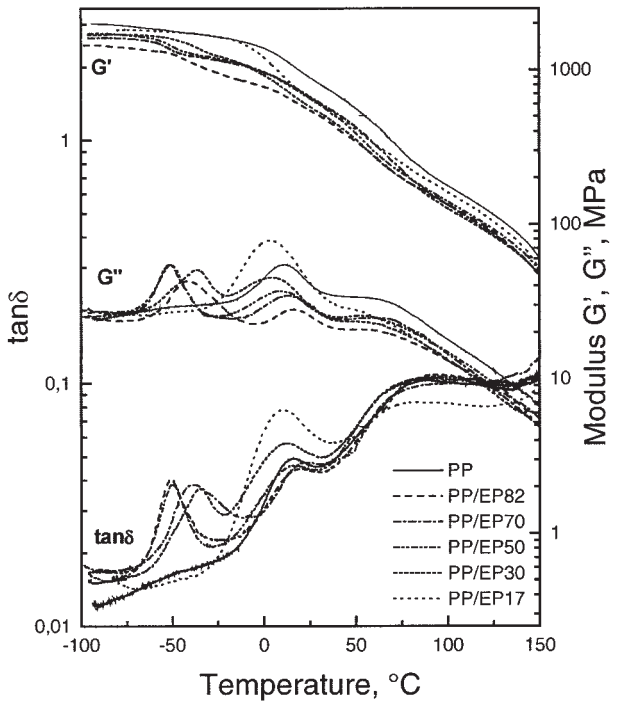

Figure 5 DMA traces of the reactor blends as a function of the EPC composition, $f = 1$ Hz.

result of the extremely high ethylene content and the slightly higher intrinsic viscosity of the EPC fraction in PP/EP82 (Table I). Both of the effects lead to a strong disparity between the viscosities of the matrix and the EPC phase and subsequently to an irregular and coarse dispersion of the latter, as will be shown by the morphology studies. Additionally, an onset of low-frequency plateau of G' was observed for PP/EP82 (Fig. 4). The appearance of such a feature in multiphase systems is commonly ascribed to the longer relaxation time of the minor phase[13,28] and corresponds to a lower deformability. Hence, it could be suggested that for the reactor blends containing ethylene-rich EPC, a phase separation takes place readily in the melt state. On the other hand, a homogeneous melt state is suggested for heterophasic EPCs with propylene-rich EPC phase as quoted also by other authors.[15,17,21]

Mechanical relaxation behavior

The mechanical relaxation profile of the reactor blends studied is revealed in Figure 5.

In the investigated temperature range, three main relaxation regions are to be discerned: (a) in the range of −50°C the α_{am} relaxation of the EPC phase (α_{am}^{EPC}), (b) in the range of 15–20°C the β relaxation of PP (β^{PP}), and (c) in the range of 80°C the α_c relaxation of PP (α_c^{PP}). The α_{am}^{EPC} and β^{PP} relaxations originate from the cooperative segmental mobility in the amor-

phous regions of the EPC and PP phase, respectively. The temperatures at which these relaxations occur are designated as glass transition temperatures of the EPC (T_g^{EPC}) and PP phase (T_g^{PP}). The α_c^{PP} relaxation is associated with molecular motions within the crystalline regions of the PP, e.g., intralamellar crystal reorientation processes, intracrystalline chain motions, or diffusion of defects within the crystalline phase.[29,30] The individual temperatures of α_{am}^{EPC}, β^{PP}, and α_c relaxation are reported to be dependent on the experimental conditions as well as on the sample preparation and treatment.[30–33]

The influence of the composition on the glass transition temperature of neat EPCs has been well investigated.[34–38] Figure 6 discloses the development of T_g^{EPC} of the studied heterophasic copolymers, in comparison to literature data of neat EPCs.

As indicated, the two curves fit reasonably well, exhibiting a minimum value at intermediate EPC compositions. An increase of the glass transition temperature is observed for higher ethylene contents. The shift is suggested to be a consequence of the restrictions, which the semicrystalline EPC fractions existing at high ethylene contents (Fig. 8) impose on the molecular motions in the amorphous regions of EPC. Thus, the T_g^{EPC} of the ethylene-rich EPC seems to refer more likely to the β transition of low density polyethylene or even to the α transition of the HDPE. The propylene-rich EPC also shows a shift of its glass transition towards higher temperatures, namely towards the glass transition temperature of the neat PP. The mutual development of T_g^{EPC} and T_g^{PP} of the investigated materials as a function of the EPC composition is demonstrated in Figure 7. As shown, decreasing ethylene content of EPC results in a simultaneous shifting of T_g^{EPC} towards higher and of T_g^{PP} towards lower temperatures, respectively.

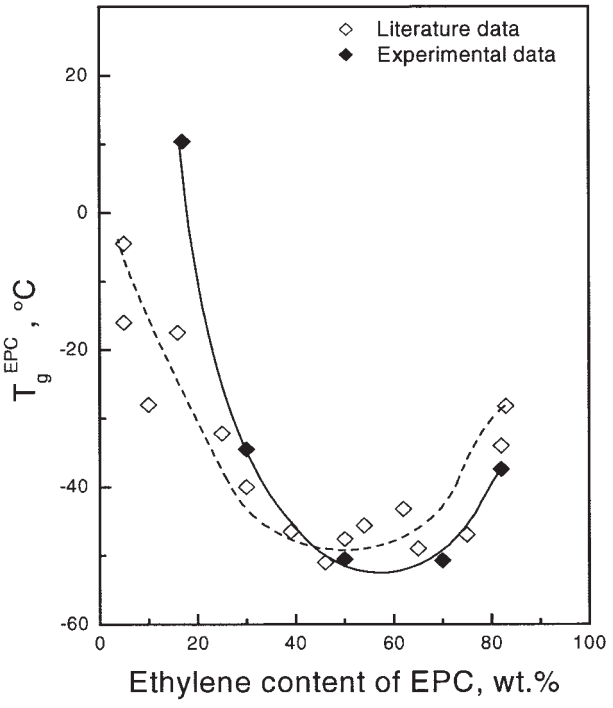

Figure 6 Effect of EPC composition on the T_g of the EPC phase (T_g^{EPC}) of the PP/EPC reactor blends as compared to literature data[29,39] of neat EPCs.

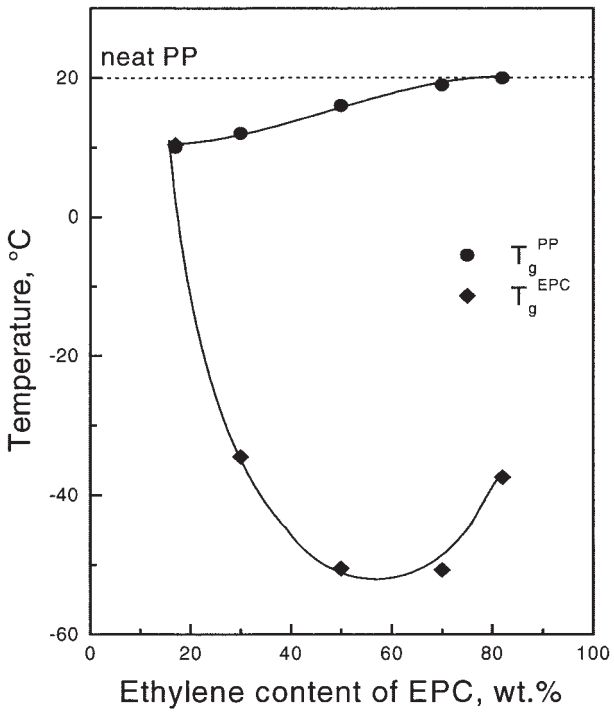

Figure 7 Glass transition temperatures of the PP (T_g^{PP}) and EPC (T_g^{EPC}) phase of the reactor blends as influenced by the EPC composition.

The degree of shifting of the both glass transition temperatures towards each other was used as an indirect measure of the extent of interaction between the blend components. Thus, according to Figure 7, an increasing propylene content of EPC leads to a stronger matrix-dispersed phase interaction. The effect is connected to a better chemical affinity between the PP matrix and the propylene-rich dispersed phase, resulting in a partial dissolution of a certain amount of propylene-rich EPC in the amorphous region between the PP lamellae. In compliance with this, an increase of the intensity of the β^{PP} relaxation was observed with increasing EPC propylene content. As pointed out in the introduction, the incorporation of a certain part of the propylene-rich EPC within the amorphous region of PP matrix was already reported for mechanical PP/EPC blends[12,18,19,21] and was supported with an observed increase of the long period.

Furthermore, T_g^{EPC} and T_g^{PP} of the material PP/EP17 having the propylene-richest EPC are found to be merged into a joint relaxation (Fig. 7). The phenom-

enon is indicative of a high extent of compatibility of the blend components. Actually, the compatibility is suggested to be additionally facilitated by the low molecular weight of EP17 (Table I). However, the T_g shifts are only a measure of the level of dispersion of the blend components or, in present systems, of the extent of dissolution of the EPC in the amorphous regions of PP. Thus, a single glass transition denotes basically a dispersed domain size below a certain value, but it is not indicative for a miscible system.[39] Indeed, the material PP/EP17, despite its single T_g, still exhibits phase separation with a size of the dispersed domains of 0.18 μm. As outlined earlier, the phase separation is suggested to be driven by the crystallization of the matrix.

Although already acquainted for blends of PP and hexene-rich ethylene–hexene copolymer[13] merged glass transition temperatures as a result of enhanced matrix-dispersed phase compatibility was quoted for PP/EPC blends only recently.[21] Nitta et al.[21] have shown that a single T_g can exist in a mechanical blend of commercial PP and an EPC with isotactic PP sequence specially synthesized with a cromium-based catalyst. In contrast, our study demonstrates the development of PP/EPC blends with high extent of matrix/dispersed phase compatibility directly in a reactor cascade over conventional ZN catalysts. Moreover, for the materials studied, merging of T_g^{EPC} and T_g^{PP} was observed irrespective of the specimen preparation method (injection or compression molding) and the thermal pretreatment.[29] The effect of enhanced matrix-dispersed phase compatibility on the fracture behavior of the heterophasic copolymers was the subject to another study.[40]

Thermal behavior

The melting and crystallization behavior of the neat PP and the resulting reactor blends as a function of the EPC composition are shown in Figure 8.

The temperatures at which crystallization and melting took place as well as the degree of crystallinity of the materials are summarized in Table III.

As indicated in Figure 8(a), all the investigated materials exhibit a main endothermic peak at a temperature of around 164°C, characteristic for the melting of the α crystalline modification of isotactic PP. The neat PP displays a shoulder at about 150°C, indicating the presence of a certain amount of β modification as well. The development of β modification is favored in slowly cooled samples.[29] The amount of β modification seems to diminish and even to disappear completely in the reactor blends. Additionally, in the heterophasic copolymers with ethylene contents ≥50 wt %, an endothermic peak in the vicinity of 120°C, characteristic for the melting of linear PE, is detected. It is ascribed to the melting of a certain amount of semi

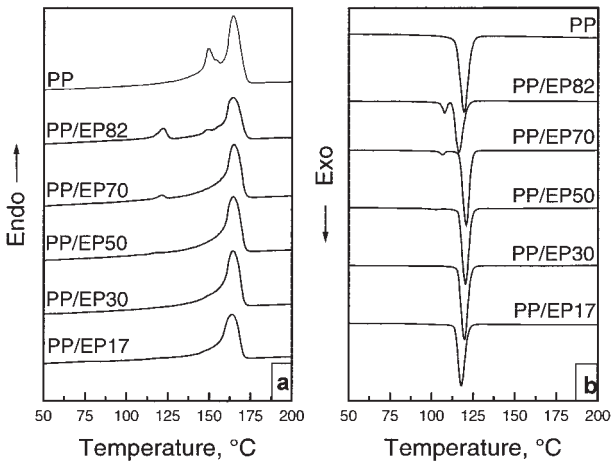

Figure 8 Melting (a) and crystallization (b) behavior of neat PP and PP/EPC reactor blends as a function of EPC composition.

cEPC possessing long crystallizable ethylene sequences. As outlined in the introduction, such a fraction is present besides the aEPC phase in reactor blends containing ethylene-rich dispersed phase. The amount of cEPC as well as the ethylene sequence length, as reflected by the peak intensity and position, respectively, was found to be increased with increasing ethylene content of the EPC. The crystallization thermograms also reveal the existence of two exothermic peaks at high ethylene contents corresponding to the separate crystallization of PP and the semicrystalline, ethylene-rich EPC phase [Fig. 8(b)]. The position of the PP melting endotherm was found to be mostly independent on the ethylene content of the dispersed phase, indicating that the thermal stability of the PP crystallites is not influenced by the presence of EPC irrespective of its composition. However, the degree of crystallinity of the PP manifests a variation with varying dispersed phase composition. As demonstrated in Table III, the X_c^{PP} was found to exhibit a maximum value at average ethylene contents of EPC. Nevertheless, the fact that in heterophasic copolymers with very high and very low ethylene content, the use of XS value as a measure of the EPC loading can cause a certain underestimation (of 20% according to Ref. 8), should be taken into account when discussing the X_c^{PP} variation. On the other hand, the same behavior was observed also by hot-stage investigations. Irrespective of the crystallization temperature, the spherulite growth rate exhibits a maximum value at intermediate ethylene content (Fig. 9).

According to theory,[41] the spherulite growth rate of PP/elastomer blends is mainly governed by the amount of energy dissipated in processes such as rejection, occlusion, deformation, and coalescence of the dispersed elastomer particles. Which of these processes will dominate is determined by the interfacial

TABLE III
Thermal Properties of the Materials as Determined from DSC

Materials	T_m^{PP} (°C)	T_m^{EPC} (°C)	T_c^{PP} (°C)	T_c^{EPC} (°C)	X_c^{PP} (%)
PP	~164	—	119	—	46
PP/EP82	~164	122	117	108	27
PP/EP70	~164	121	121	107	34
PP/EP50	~164	118	119	102	37
PP/EP30	~164	—	120	—	35
PP/EPI7	~164	—	118	—	28

tension between the matrix and the dispersed phase, the viscosity of the components, the size of the elastomer domains, and the crystallization conditions.

For the heterophasic copolymers subject to this study, two limiting cases can be discussed. As shown by the DMA investigations (Fig. 7), PP/EP17 represents a system with high extent of matrix/dispersed phase compatibility (low interfacial tension). This system is of low viscosity and is suggested to give a rise of a homogeneous melt, whereas phase separation occurs upon the crystallization of PP. According to the theoretical calculations,[41] in such compatible systems, a rejection of the noncrystallizable minor component into interlamellar regions of the spherulites and/or in the interspherulitic regions takes place during the crystallization process. This behavior is also suggested for material PP/EP17. As a result, the spherulite structure of PP/EP17 appears very similar to those of the neat PP [Fig. 10(b)].

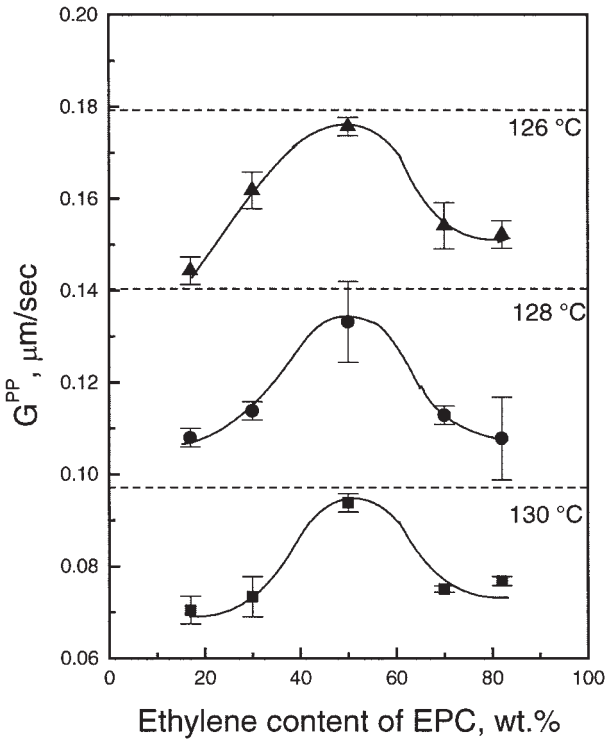

Figure 9 Spherulite growth rate of the PP (G^{PP}) as a function of EPC composition at a crystallization temperature (T_c) of (■) 130°C, (●) 128°C, and (▲) 126°C. The dashed lines represent spherulite growth rate of the neat PP at the corresponding temperatures.

Thus, the substantial decrease of the spherulite growth rate in PP/EP17 (Fig. 9) is attributed from one side to the energy dissipated in the rejection of the elastomer particles by the growing PP crystals. On the other side, because of its dissolution in the amorphous regions of PP, the EP17 is acting like a diluent of the crystallizable PP fraction. The results concur with the studies of other research groups.[17,21,42] Additionally, a significant depression of the primary nucleation density of PP has been reported in PP/EPC blends with high extent of matrix/dispersed phase compatibility.[43] The G^{PP} drop is in accordance with the decrease of the X_c^{PP}. Moreover, long propylene sequences of EP17 are assumed to participate in the crystallization process of PP and probably to be incorporated in the PP crystal lattice.[21] This is implied by the increased width at half height of the melting peak of PP/EP17 indicative for broadening of the lamellae thickness distribution as well as by the morphological investigation.

At the other concentration edge, the specific rheological behavior of PP/EP82 and the grained structure of the melt observed in polarized light suggest a phase separation of the blend components readily in the melt state. This is predisposed mainly by interfacial energy reasons. Thus, occlusion of the EPC particles by the growing spherulites and their subsequent deformation is assumed. Because of the higher viscosity and coarser dispersion of the ethylene-rich EPC phase, the PP spherulites are unable to deform it and push it in the interspherulitic regions.[44,45] This results in a highly irregular spherulitic structure as shown in Figure 10(d). In accordance to the theoretical considerations, this spatial hindrance causes a decrease of the spherulite growth rate and consequentially in the X_c^{PP}.

Finally, at a E_c^{EPC} of ~50 wt % [Fig. 10(c)], the spherulite growth rate of the heterophasic copolymers is almost identical with those of the PP matrix, representing a balance between compatibility and viscosity effects.

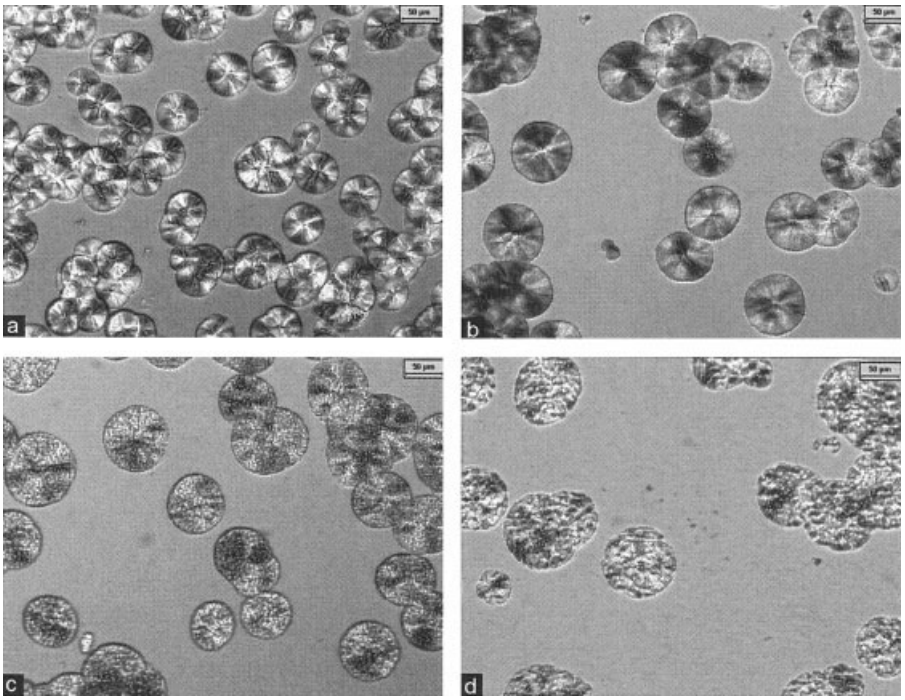

Figure 10 Optical micrographs of the spherulite texture at 128°C: (a) neat PP; (b) PP/EP17; (c) PP/EP50; (d) PP/EP82.

Morphology

The SEM micrographs of the heterophasic copolymers with respect to the EPC composition are presented in Figure 11.

As shown, the overall blend morphology as well as the internal morphology of the composite dispersed phase particles is highly influenced by the EPC composition. Figure 12 displays the diameter of the dispersed domains as a function of EPC composition. Considering the "tomato-cut" problem, the maximum particle diameter, which approximates most closely the true particle diameter, is included as well.

Despite the different absolute values, the same trend for decreasing dispersed domain size with decreasing ethylene content of the EPC is demonstrated. The effect is ascribed from one side to the high degree of solubility of the propylene-rich EPC in the amorphous region between PP lamellae and from the other side to the decreased interfacial tension between the matrix and the high propylene containing EPC.[46] It should be emphasized that a reduction of several orders of magnitude of the size of the dispersed EPC particles took place, especially pronounced at the concentration extremes, i.e., at very high and very low ethylene contents of the EPC (Fig. 12). Consistent with the demonstrated rheological properties, the material PP/EP82 exhibits a very coarse dispersion [Fig. 11(a)]. At the other concentration edge, the EPC with the highest propylene content organizes itself in a very fine dispersion [Fig. 11(e)]. The domains are regularly distributed by both shape and size, suggesting that by the rapid cooling during injection molding process, the EPC phase is rejected preferentially in the interlamellar regions of the PP spherulites. The phenomenon is associated to the high degree of compatibility between the matrix and the propylene-rich dispersed phase as indicated by the single glass transition temperature that this material exhibits.

Parallel with the variation of the dispersed domain size, the EPC microstructure varies with the EPC composition as well. The heterophasic materials with an ethylene content below 50 wt % [Fig. 11(d–e)] exhibit only empty embeddings, indicating where the EPC particles originally resided. It is assumed that the dispersed phase is completely dissolved during the etching procedure. However, at higher ethylene contents, composite EPC particles comprised of amorphous shell with incorporated semicrystalline inclusions of cEPC are to be observed [Fig. 11(a–c)]. For the materials PP/EP50 and PP/EP70, mainly two types of structure could be discerned. Smaller particles exhibit a core–shell structure with a single inclusion while a "salami-like" structure with multiple inclusions is characteristic for the larger particles. It is suggested that the larger particles are formed predominantly as a result of coalescence processes of the smaller particles.[47] The number and size of the inclusions were found to correlate with the ethylene content of EPC. Further on, the material with the highest ethylene content (PP/EP82) displays a completely different internal structure of the modifier particles [Fig. 11(a)]. A similar internal structure of the dispersed phase do-

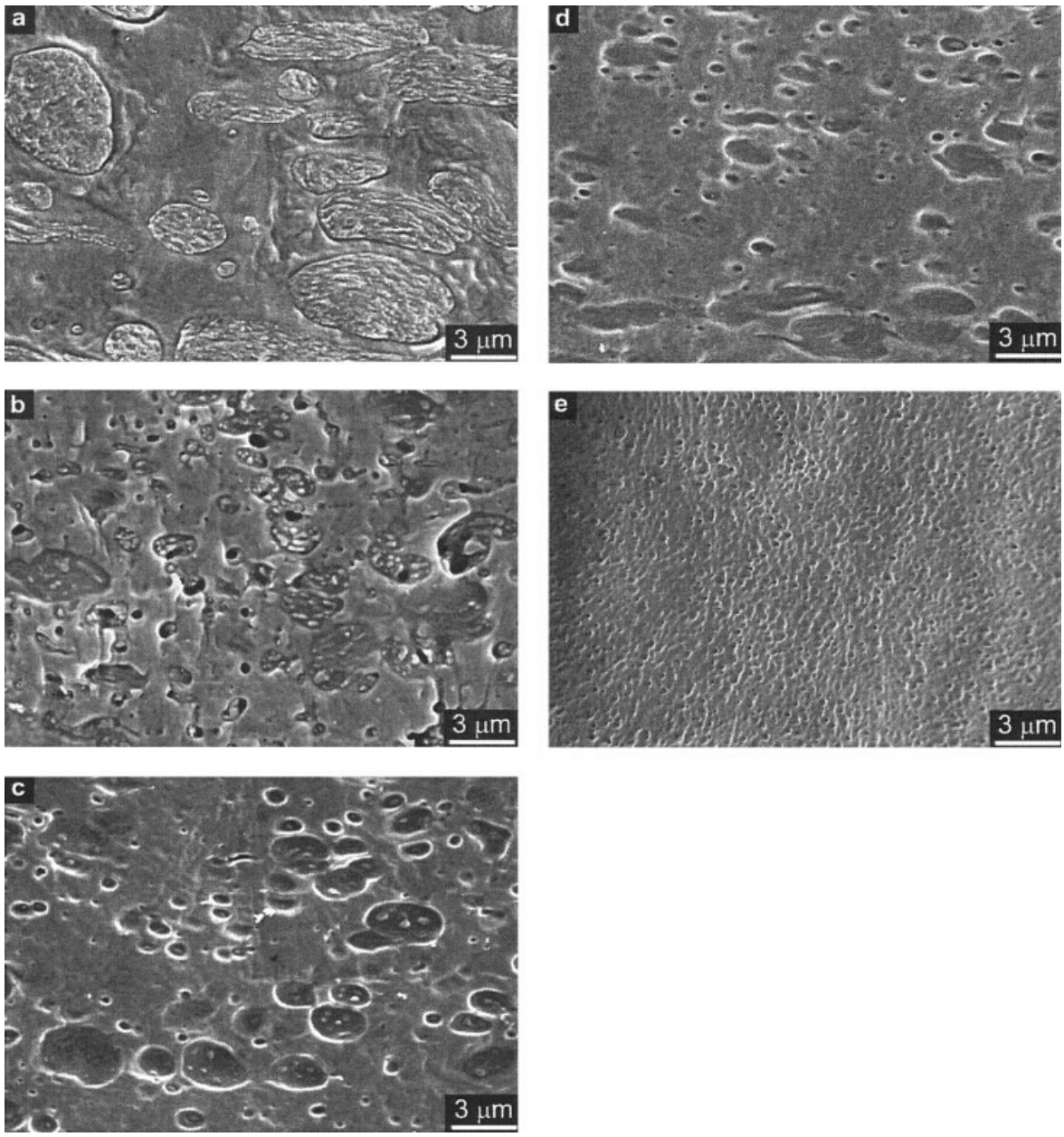

Figure 11 SEM micrographs of the materials (a) PP/EP82, (b) PP/EP70, (c) PP/EP50, (d) PP/EP30, (e) PP/EP17.

mains has been observed in PP/EPC/HDPE mechanical blends with high HDPE content[48,49] and designated by Stehling et al.[49] as an interpenetrating. However, in the case of the reactor blends studied, a phase separation within the dispersed domains is still to be discerned. Both the small and the large EPC domains manifest a core–shell structure with a large core of semicrystalline EPC surrounded by a thin layer of aEPC shell. For more detailed characterization of the internal structure of the dispersed domains, transmission electron microscopy (TEM) was employed. TEM micrographs of the materials PP/EP82 and PP/EP17 are presented in Figures 13 and 14, respectively. Because of the applied staining procedure, the amorphous part of the EPC particles appears dark, while the PP matrix and the semicrystalline EPC inclusions appear bright. As shown, there is a high consistency of the reactor blend morphology obtained by means of TEM and SEM, suggesting that SEM with the utilized etching technique offers an attractive and relative simple approach for morphology characterization. However, the TEM gives more insight, revealing the structure of the investigated heterophasic copolymers down to a lamellar level. In Figure 13, the typical cross-hatched pattern of the isotactic PP is demonstrated, consisting of superimposed radial and tangential lamellae. Furthermore, the internal structure of the large semicrystalline core of PP/EP82 is also disclosed

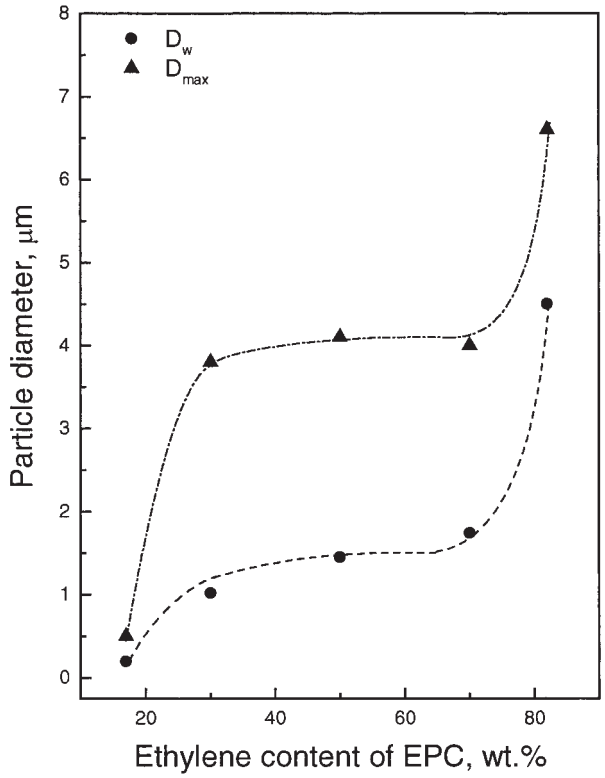

Figure 12 Weight average (D_w) and maximum (D_{max}) diameter of the dispersed particles, evaluated on the SEM micrographs, as a function of EPC composition.

in detail. The core is composed of PE crystalline lamellae originating from EPC fractions possessing long ethylene sequences. Considering the lamellae thickness, it is suggested that almost a linear PE fraction is present in the material PP/EP82. This fact is in accordance with the position of the endotherm corresponding to the melting of the semicrystalline EPC phase as measured by DSC (Fig. 8). Besides the PE crystalline lamellae, some amorphous material is found to be

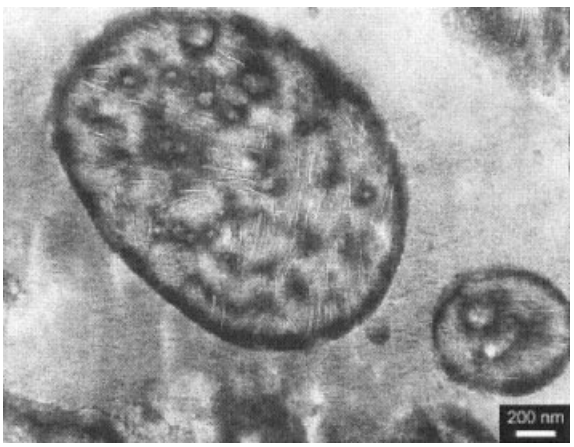

Figure 13 Internal domain structure of PP/EP82.

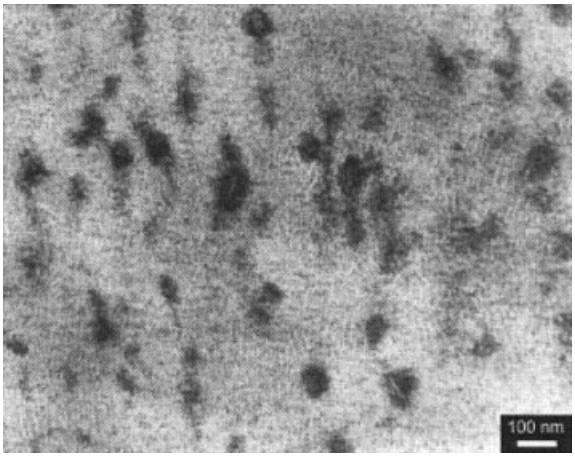

Figure 14 TEM micrograph of the material PP/EP17.

entrapped in the core as well. Further on, the fine morphology of PP/EP17 is presented in Figure 14. A rather blurred interface is observed between the PP matrix and the propylene-rich dispersed phase in comparison to PP/EP82. It is attributed to the strong matrix-dispersed phase interactions and interfacial adhesion in this material. A closer look on the dispersed phase internal morphology reveals also the existence of lamella-like structures within the EPC particles, however not so pronounced as in the PP/EP82 material. They appear to be of the same thickness as the matrix lamellae and to be interconnected to some degree with the same. Taking into account the very high propylene content of the EPC, it is assumed that the observed structures are a result of the crystallization process of long propylene sequences of the dispersed phase.

A schematic illustration of the morphology as well as of the microstructure development of the dispersed domains as a function of the EPC composition has been proposed in Figure 15.

CONCLUSIONS

In the present study, the phase interactions and the structure evolution of *in situ* produced PP/EPC blends have been investigated as influenced by the EPC composition. It was demonstrated that the EPC composition (ethylene/propylene ratio) governs primarily the extent of matrix-dispersed phase compatibility of the reactor blends. An increase of the propylene content of the EPC was found to enhance significantly the compatibility of the blend components as evaluated by the glass transition temperature shifts. Moreover, at EPC ethylene content of 17 wt %, the glass transition temperatures of the both phases were shown to merge into a joint relaxation peak. The result manifests a high degree of compatibility between the phases, which is assumed to be facilitated also by the lower molecular

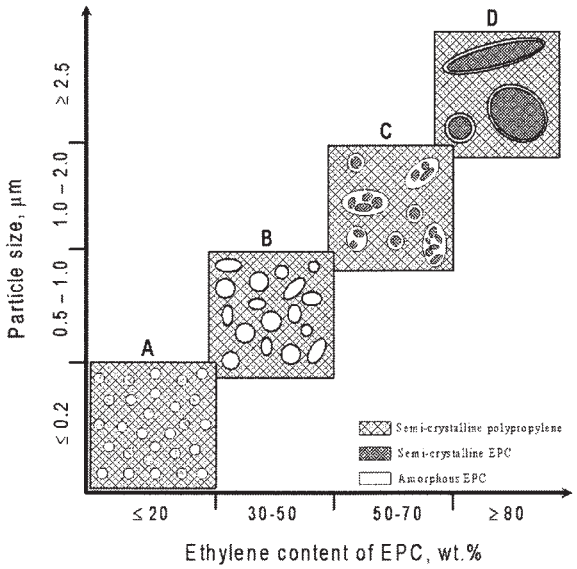

Figure 15 Morphology development of heterophasic EPCs. A: Fine dispersed EPC domains with PP crystallinity; B: aEPC domains; C: coexistence of core–shell and "salami-like" EPC domains; D: coarse EPC domains of core–shell structure.

weight of EPC phase. The EPC composition was found to influence the morphology development of the reactor blends. It was shown that at constant viscosity of the matrix, the ethylene content of the EPC dominates the viscosity ratio as well as the interfacial tension between the matrix and the dispersed phase, and consequentially the size and microstructure of the EPC domains. A reduction of the particle size with several orders of magnitude was observed with increasing propylene content of the EPC. The results correlate to the extent of compatibility, i.e., to the extent of dissolution of the propylene-rich EPC in the amorphous region of the PP matrix. At ethylene contents higher than 50 wt %, composite EPC particles comprised of amorphous shell and polyethylene-like, semicrystalline inclusions have been discerned. Very high ethylene content of the EPC causes a strong disparity between the viscosities of the matrix and the EPC inducing the development of a specific type of core–shell structure. Further on, it was demonstrated that the crystallization behavior and spherulite growth of PP matrix were influenced by the dispersed phase composition. For the studied reactor blends, it was stated that with increasing ethylene content of EPC, a transition from rejection to occlusion and subsequent deformation of the dispersed particles by the growing PP spherulites takes place. The energy dissipated in these processes influences the spherulite growth rate and the degree of crystallinity of the PP matrix. The highest spherulite growth rate and degree of crystallinity were observed for the heterophasic materials of intermediate ethylene content.

The authors thank D. Wulff and W. Bohnenberger at Dow Olefinverbund GmbH (Schkopau, Germany) for preparation of the materials and accomplishment of the rheological measurements, respectively.

References

1. Van der Ven, S. Polypropylene and Other Polyolefins; Elsevier: New York, 1990; p 268.
2. Albizzati, E. In Polypropylene Handbook; Moore E. P., Ed.; Carl Hanser: Munich, 1998; p 89.
3. Mirabella, F. Polymer 1993, 34, 1729.
4. Zagur, R.; Goizueta, G.; Capiati, N. Polym Eng Sci 1999, 39, 921.
5. Kamfjord, T.; Stori, A. Polymer 2001, 42, 2767.
6. Pires, M.; Mauler, R.; Liberman, A. J Appl Polym Sci 2004, 92, 2155.
7. Hongjun, C.; Xiaolie, L.; Dezhu, M.; Jianmin, W.; Hongsheng, T. J Appl Polym Sci 1999, 71, 93.
8. Randall, J. C. J Polym Sci Part A: Polym Chem 1998, 36, 1527.
9. Fan, Z.; Zhang, Y.; Xu, J.; Wang, H.; Feng, L. Polymer 2001, 42, 5559.
10. Cecchin, G. Macromol Symp 1994, 78, 213.
11. Hongjun, C.; Xiaolie, L.; Dezhu, M.; Jianmin, W.; Hongsheng, T. J Appl Polym Sci 1999, 71, 103.
12. Yamaguchi, M.; Miyata, H.; Nitta, K.-H. J Appl Polym Sci 1996, 62, 87.
13. Yamaguchi, M.; Nitta, K.-H.; Miyata, H.; Masuda T. J Appl Polym Sci 1997, 63, 467.
14. Lohse, D. Polym Eng Sci 1986, 26, 1500.
15. Seki, M.; Nakano, H.; Yamauchi, S.; Suzuki, J.; Matsushita, Y. Macromolecules 1999, 32, 3227.
16. Greco, R.; Mancarella, C.; Martuscelli, E.; Ragosta, G.; Jinghua, Y. Polymer 1987, 28, 1929.
17. Greco, R.; Martuscelli, E.; Ragosta, G.; Jinghua, J. J Mater Sci 1988, 23, 4307.
18. Nomura, T.; Nishio, T.; Fujii, T.; Sakai, J.; Yamamoto, M.; Uemura, A. Polym Eng Sci 1995, 35, 1261.
19. D'Orazio, L.; Mancarella, C.; Martuscelli, E.; Sticotti, G. J Mater Sci 1991, 26, 4033.
20. Van der Ven, S.; Polypropylene and Other Polyolefins; Elsevier: New York, 1990; p 289.
21. Nitta, K.-H.; Shin, Y.-W.; Hashiguchi, H.; Tanimoto, S.; Terano, M. Polymer 2005, 46, 965.
22. Brandup, J.; Immergut, E. H.; Polymer Handbook, 3rd ed.; Wiley: New York, 1989; p 268.
23. Olley, R. H.; Hodge, A. M.; Bassett, D. C. J Polym Sci Part A-2: Polym Phys 1979, 17, 627.
24. Yasuda, K.; Armstrong, R. C.; Cohen, C. E. Rheol Acta 1981, 20, 63.
25. D'Orazio, L.; Mancarella, C.; Martuscelli, E. Polymer 1991, 32, 1186.
26. Mighri, F.; Huneault, M. A.; Ajji, A.; Ko, G. H.; Watanabe, F. J Appl Polym Sci 2001, 82, 2113.
27. Tsenglou, C. J Polym Sci Part A: Polym Phys 1988, 26, 2329.
28. Gahleitner, M. Prog Polym Sci 2001, 26, 895.
29. Doshev, P.; Kolesov, I.; Androsch, R.; Lohse, G.; Radusch, H.-J. Proceedings of Polymeric Materials, Halle/Saale, Germany, September 29–October 01, 2004.
30. Jourdan, C.; Cavaille, J. Y.; Perez, J. J Polym Sci Part A: Polym-Phys 1989, 27, 2361.
31. Boyd, R. Polymer 1985, 26, 323.
32. Amash, A.; Zugenmaier, P. J Polym Sci Part A: Polym Phys 1997, 35, 1439.
33. Murayama, T. Dynamic Mechanical Analysis of Polymeric Materials, Monograph; Elsevier: New York, 1978; p 89.
34. Maeder, D.; Heinemann, J.; Walter, P.; Muelhaupt, R. Macromolecules 2000, 33, 1254.
35. Van der Ven, S. Polypropylene and Other Polyolefins; Elsevier: New York, 1990; p 254.

36. McCrum, M. G.; Read, B. E.; Williams, G. Anelastic and Dielectric Effects in Polymeric Solids; Dover Publications Inc.: New York, 1993; p 376.
37. Shin, Y.; Uozumi, T.; Terano, M.; Nitta, K. Polymer 2001, 42, 9611.
38. Nitta, K.; Kawada, T.; Yamahiro, M.; Mori, H.; Terano, M. Polymer 2000, 41, 6765.
39. Utracki, L. Polymer Alloys and Blends; Carl Hanser: Munich, 1989; p 93.
40. Doshev, P.; Lach, R.; Lohse, G.; Heuvelsland, A.; Grellmann, W.; Radusch, H.-J. Polymer, to appear.
41. Bartczak, Z.; Galeski, A.; Martuscelli, E. Polym Eng Sci 1984, 24, 1155.
42. Yamaguchi, M.; Miyata, H.; Nitta, K.-H. J Polym Sci Part A: Polym Phys 1997, 35, 953.
43. Bartczak, Z.; Galeski, A.; Martuscelli, E.; Jnik, H. Polymer 1985, 26, 1843.
44. Martuscelli, E.; Pracella, M.; Della Volpe, G.; Greco, P. Makromol Chem 1984, 185, 1041.
45. Martuscelli, E.; Pracella, M.; Della Volpe, G.; Greco, P. Makromol Chem 1980, 181, 957.
46. Menke, T. Ph.D. Thesis, Martin Luther University Halle-Wittenberg, Halle/Saale, Germany, 2001.
47. Zagur, R.; Goizueta, G.; Capiati, N. Polym Eng Sci 2000, 40, 1921.
48. Hauer, A.; Bernreitner, K.; Ignolic, E.; Gahleitner, M. Proceedings of 18th Annual Meeting of the Polymer Processing Society, Guimaraes, Portugal, June 16–20, 2002.
49. Stehling, F.; Huff, T.; Speed, C. S.; Wissler, G. J Appl Polym Sci 1981, 26, 2693.